



Faculty of Technology and Science  
Materials Engineering

---

Vitaliy Kazymyrovych

# Very high cycle fatigue of engineering materials

(A literature review)

Vitaliy Kazymyrovych

# Very high cycle fatigue of engineering materials

(A literature review)

Vitaliy Kazymyrovych. *Very high cycle fatigue of engineering materials - A literature review*

Research Report

Karlstad University Studies 2009:22

ISSN 1403-8099

ISBN 978-91-7063-246-4

© The Author

Distribution:

Faculty of Technology and Science

Materials Engineering

SE-651 88 Karlstad

+46 54 700 10 00

[www.kau.se](http://www.kau.se)

Printed at: Universitetsstryckeriet, Karlstad 2009

# **Very high cycle fatigue of engineering materials**

## **(A literature review)**

*V.Kazymyrovych\**

*Department of Materials Engineering, Karlstad University SE-651 88, Sweden*

*\* Email address: Vitaliy.Kazymyrovych@kau.se*

### **Abstract**

This paper examines the development and present status of the Very High Cycle Fatigue (VHCF) phenomenon in engineering materials. The concept of ultrasonic fatigue testing is described in light of its historical appearance covering the main principles and equipment variations. The VHCF behaviour of the most important materials used for very long life applications is presented, with particular attention paid to steels. In section 3 the VHCF properties of titanium-, nickel-, aluminium- and magnesium alloys are described. Furthermore, the typical fatigue behaviour and mechanisms of pure metals are presented. Section 4 examines the VHCF properties of various types of steels e.g. low carbon steel, spring steel, stainless steel, bearing steel as well as tool steel.

In addition to this, the main material defects that initiate VHCF failure are examined in this study. Furthermore, the different stages characteristic for fatigue crack development in VHCF are described in section 5 in terms of relative importance and sequence. Finally, a few fatigue crack evolution models, including hydrogen assisted crack growth as well as carbide decohesion model, are presented in section 6. The literature review is concluded by the challenges and ambiguities that surround the area of VHCF and the directions for the future work are identified.

## 1. Introduction

The word *fatigue* is derived from the Latin *fatigare* which means “to tire”. In engineering terminology *fatigue* is a progressive structural damage of materials under cyclic loads. There are a few main types of fatigue. *Mechanical fatigue* is the focus of this study and could be described as damage induced by application of fluctuating stresses and strains. Among other types of fatigue are: *creep fatigue* – cyclic loads at high temperatures; *thermal fatigue* – cyclic changes in material’s temperature; thermo-mechanical fatigue – a combination of mechanical and thermal fatigue; *corrosion fatigue* – cyclic loads applied in chemically aggressive or embrittling environment; *fretting fatigue* – cyclic stresses together with the oscillation motion and frictional sliding between surfaces. The devastating power of the fatigue phenomenon is underlined by the fact that very often final fatigue failure occurs at stresses that are well below the yield point of the material.

*Fatigue life* is an important characteristic of an engineering component and is measured by a number of cycles it can withstand before fatigue failure takes place. Based on the fatigue life concept the mechanical fatigue could be sub-divided into: *low cycle fatigue* (LCF) – up to  $10^6$  cycles to failure; *high cycle fatigue* (HCF) – between  $10^6$  and  $10^8$  cycles to failure and *very high cycle fatigue* (VHCF) – over  $10^8$  cycles to failure. The VHCF represents the main point of interest in this study.

With the progress in technological development the required fatigue life for many components has increased to exceed  $10^8$  load cycles. Nowadays the VHCF constitutes one of the main design criteria for a number of applications in aircraft, automobile, railway and other industries. Some examples of such components are: gas turbine disks ( $10^{10}$ ), car engine cylinder heads and blocks ( $10^8$ ), ball bearings, high frequency drilling machines, diesel engines of ships and high speed trains ( $10^9$ ), etc.

Even though a large amount of fatigue data is available in the form of S-N curves, these results are often limited to  $10^7$  load cycles, after which the material is often considered to have unlimited life. Such an assumption of fatigue limit (maximum stress at which material can sustain unlimited number of cycles) was satisfactory enough in the past when engineering components were not expected to endure more than  $10^7$  load cycles. In view of the present technological developments VHCF of materials has become a topic of significant interest. It is important to know with a good degree of certainty the fatigue behaviour of a material when it is subjected to  $10^8 - 10^{10}$  load cycles, whether it has a fatigue limit or exhibits continuously decreasing stress-life response. This ambiguity could be removed by the means of experiment. Time and cost constraints hinder the use of conventional fatigue testing in the VHC range. Instead, piezoelectric fatigue machines evolved, which enabled efficient and reliable testing in the desired VHC range. They are capable of producing  $10^{10}$  cycles in less than one week (at 20 kHz) while it would take more than three years for the same experiment using conventional equipment.

Early experiments using the above equipment show that most materials do not have a fatigue limit at  $10^7$  cycles but instead their fatigue strength gradually decreases as fatigue life reaches  $10^8 - 10^{10}$  load cycles. Therefore, the concept of fatigue limit is not adequate and it would be

more appropriate to talk about fatigue strength at a certain number of cycles. Hence, there is a need for the establishment of reliable fatigue diagrams for different materials extending into VHCF range. Moreover, considerable attention is devoted to the fatigue crack initiation and propagation mechanisms that are activated when a material is subjected to VHCF.

This paper intends to summarize the present developments in the field of VHCF. The concept of ultrasonic fatigue testing is described in the next section. It is followed by the VHCF data of selected materials and a relating discussion. Then focus of is shifted to the VHCF behavior of steels as the most important structural material. The mechanisms and stages of fatigue crack initiation and growth in the VHCF regime are examined. Here the crucial role of materials' internal defects such as inclusions, carbides and voids in the formation of fatigue cracks is emphasized. Both initiation and growth of fatigue cracks are important in understanding VHCF, however, the prime importance of crack initiation stage, with respect to the fatigue life, is stressed. The paper is concluded by presenting different fatigue models that are claimed to represent VHCF behavior of various materials.

## 2. Testing method

The aim of fatigue testing is to establish fatigue strength - the materials' ability to withstand cyclic loading. If a material is cyclically loaded it means it experiences repetitive loading of a certain character, which in most cases is either bending, torsion, tensile loading or a combination of the above mentioned types. A load cycle is characterised by a *load ratio*  $R = \text{minimum load } (\sigma_{\min}) / \text{maximum load } (\sigma_{\max})$ ; and stress amplitude  $\sigma_a = (\sigma_{\max} - \sigma_{\min})/2$ . In this paper only the fatigue results with constant amplitude loading are discussed. Other parameters describing cyclic testing are *mean stress*  $\sigma_m = (\sigma_{\max} + \sigma_{\min})/2$  and *stress range*  $\Delta\sigma = \sigma_{\max} - \sigma_{\min}$  (Fig. 1).

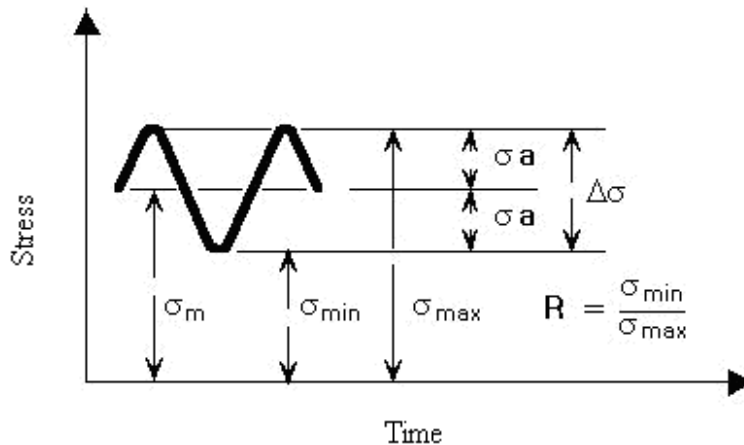


Figure 1. Stress parameters used to define constant amplitude loading.

*Fatigue strength* is best defined at a certain number of cycles and could be presented in the form of “stress – number of cycles” (S-N) curve, established by experiments (Fig. 3-10). Fatigue strength with reference to a certain number of load cycles describes a stress level at which there is a 50 % probability that a material will fail due to fatigue damage. In contrast to

fatigue strength, a *fatigue limit* is a stress level below which no fatigue failure is expected regardless of the number of load cycles endured by the material.

With respect to VHCF one of the main tasks is to investigate whether or not a fatigue limit exists for different materials as well as to establish their fatigue strengths at  $10^7$  and higher number of load cycles.

### ***Ultrasonic fatigue testing***

As mentioned earlier the conventional fatigue testing does not have practical capability to provide fatigue results in the VHC range. This could be successfully accomplished using ultrasonic fatigue test machine, which is the focus of this section. The frequency of ultrasonic fatigue testing ranges from 15 to 30 kHz with the typical one being 20 kHz. This offers drastic decrease in time and subsequently cost of fatigue testing, Table 1.

Table 1  
Ultrasonic versus conventional fatigue testing.

Number of cycles	Ultrasonic (20 kHz)	Conventional (100 Hz)
$10^7$ cycles	9 minutes	1 day
$10^9$ cycles	14 hours	4 months
$10^{10}$ cycles	6 days	3 years

The concept of ultrasonic fatigue testing was initiated at the beginning of the 20th century by Hopkinson who developed the first electromagnetic resonance system of 116 Hz. At that time the highest attainable fatigue testing frequency of a mechanically driven system was 33 Hz. Then in 1925 Jenkin applied similar technique to test copper, iron and steel wires at the frequency of 2.5 kHz. Later in 1929 together with Lehmann he produced pulsating air resonance system and reached the frequency of 10 kHz. In 1950 Mason marked an important development in the ultrasonic fatigue testing technique. He introduced piezo-electric transducers that transformed 20 kHz electrical signals into mechanical vibrations of the same frequency. Mason made use of high power ultrasonic waves to induce materials fracture by fatigue. Afterwards even higher frequencies for fatigue testing were reached by Girald (1959, 92 kHz) and Kikukawa (1965, 199 kHz). However, the prototype of Manson's 20 kHz machine is used as a basis for most modern ultrasonic fatigue testing equipment.

Since the first ultrasonic fatigue machine was constructed by Mason in 1950, with the development of computer sciences, several laboratories have developed their own machines and designed practical test procedures. Laboratories of Willertz in the US, Stanzl in Austria, Bathias in France, Ishii in Japan and Puskar in Slovakia, are among leading laboratories in this field.

Starting from early 80th many researches published important works based on the results of ultrasonic fatigue testing. Many of them will be referred to or briefly presented in the course of this paper.

The development of ultrasonic equipment in combination with demand for VHCF properties of different materials led to the increased interest in ultrasonic fatigue testing. Ultrasonic fatigue testing technology provides a time saving and economical method to obtain fatigue data in the very high cycle regime. Besides, it offers a reliable way of testing at the extremely small rates of crack growth in the threshold regime

Following is the short description of the ultrasonic fatigue testing equipment.

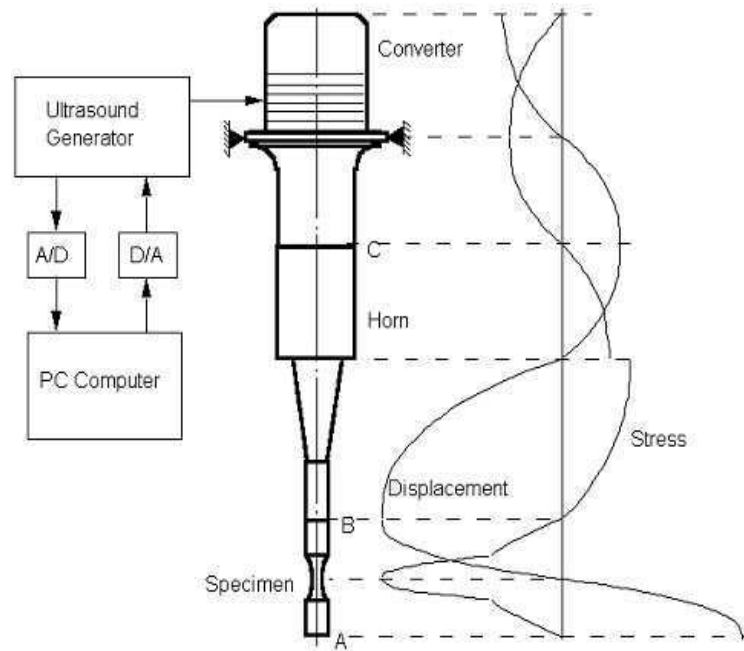


Figure 2. Ultrasonic fatigue test system and stress-displacement field.

Due to the lack of standardization the ultrasonic test machines differ from laboratory to laboratory, but we can distinguish the following main components that are common to all of them, Fig. 2:

1. A power generator that transforms 50 or 60 Hz voltage signal into 20 kHz ultrasonic electrical sinusoidal signal.
2. A piezoelectric converter excited by the power generator, which transforms the electrical signal into longitudinal ultrasonic waves and mechanical vibration of the same frequency.
3. An ultrasonic horn that amplifies the vibration coming from the converter in order to obtain the required strain amplitude in the middle section of the specimen.

The specimen, horn and converter form a mechanical resonance system with four stress nodes (zero stress) and three displacement nodes (zero displacement) at an intrinsic frequency of 20 kHz. As could be seen from Fig. 1 the maximum stress is in the specimen's centre, which is one of the displacement nodes, while the displacement reaches its maximum at the specimen's ends (points A and B). The above three parts are essential for the production of ultrasonic fatigue load. Other components of the ultrasonic fatigue test machine may include recording

systems (amplitude and control units, cycle counter, oscilloscope etc.) and measuring systems (displacement sensor, video-camera).

During ultrasonic fatigue testing due to the effect of internal friction, the specimen's temperature can significantly increase. This would have influenced the fatigue behaviour of tested material. Therefore, the specimen should be cooled with clean and dry compressed air. In order to maximize the effect of cold air the adjustable gun should be installed.

The setup presented in Fig. 1 allows fatigue testing with the load ratio  $R = -1$ . In order to obtain another load ratio an additional horn, identical to the first one, is attached to the bottom of a specimen. Tensile pre-stress is then applied to the specimen, which is followed by superposing of an ultrasonic load.

The progress in ultrasonic testing made during the last two decades enables fatigue testing with variable amplitude loading conditions, at different temperatures and in variety of environments. In addition to this, using ultrasonic technique, it is now possible to evaluate fatigue properties of materials in terms of torsion, bending, fretting or multi-axial loading.

### **3. VHCF of materials**

The VHCF behaviour varies from material to material and its accurate prediction based on some theoretical models is so far unattainable. Therefore, the experimental data for different materials, which was generated mainly over the last decade, is of great importance. The results show that some materials display a fatigue limit at typically  $10^6$ - $10^7$  load cycles, while most others do not exhibit this response, showing gradual decrease in fatigue strength when number of cycles reaches into giga-cycle range.

With respect to VHCF properties the materials could be categorized into two classes: type I and type II materials. For the first class of materials the difference between the fatigue strength at  $10^6$  and  $10^9$  cycles is less than 50 MPa (1). To this category belong ductile homogeneous single-phase metals (copper and nickel are typical representatives) and some alloys. Low carbon steels, some stainless steels and spheroid graphite cast iron also present such behaviour. The type II materials exhibit fatigue strength decrease at  $10^9$  cycles compared to  $10^6$  cycles in the range of 50-300 MPa. This class covers mainly high-strength steels and other materials containing heterogeneities in the form of inclusions, pores, coarse second phase particle, all of which could act as internal fatigue crack initiation sites. It appears that the higher the ultimate tensile strength (UTS) of a material, the steeper is the S-N curve in the giga-cycle range.

In this section the attempt is made to present an overview of the available VHCF data for different materials with some discussion around it. Among the materials which are often studied by VHCF testing are ferrous materials, titanium alloys, nickel alloys, aluminum alloys and polycrystalline copper. These materials are widely used in aeronautics, aerospace, automotive, railway and other industries. They constitute the base for manufacturing components that operate in VHCF conditions.

In this section the focus of attention is shifted towards materials other than steels, which will be treated in more details in the next section.

### ***VHCF of titanium alloys***

Titanium alloys play very important role in aerospace industry, where VHCF is a common phenomenon. It is generally believed that in giga-cycle fatigue their behaviour resembles that of steels (1).

Fig. 3 shows the S-N behaviour for 6246 titanium alloy tested at 20 kHz at room temperature. The material was forged and subjected to different heat treatments 1-3, which resulted in significant difference in fatigue strength. For the heat treatments details readers are referred to (2), but it should be pointed out that the best fatigue strength at  $10^9$  load cycles is achieved with heat treatments producing larger volume fraction of secondary  $\alpha$  and small platelets of primary  $\alpha$ . The following conclusions have been drawn in (2) from the test results:

- There is no fatigue limit
- The fatigue strength at  $10^9$  cycles is much smaller than at  $10^6$  load cycles.
- The microstructure has a great influence on the fatigue strength.

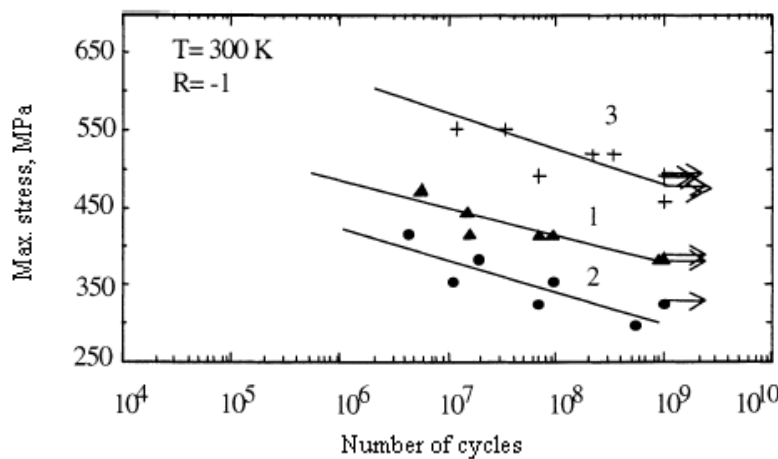


Figure 3. S-N curves for Ti6246 alloy with different heat treatments 1-3 (2).

Another example is T6A4V titanium alloy, which was tested by C. Bathias et. al. (1) at frequency 20 kHz and load ratio  $R = -1$ . The results are presented in Fig. 4 together with additional data obtained in other laboratories during testing at 20 and 100 Hz. It could be seen that the fatigue behavior of T6A4V alloy in VHCF regime is better than that observed during traditional fatigue testing at lower frequencies. Furthermore, Fig. 4 suggests that in terms of fatigue strength the material does not degrade a lot with increasing number of cycles when tested in VHCF range.

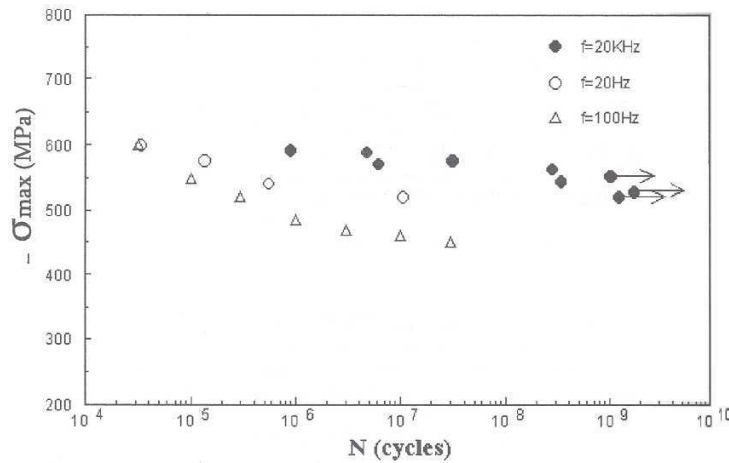


Figure 4. S-N curve for T6A4V alloy (1)

### *VHCF of nickel alloys*

The large family of nickel alloys has extensively been used for high performance applications such as, for example, gas turbine blades and turbocharger rotors. Therefore, some research has been done with respect to VHCF behaviour of these alloys. C. Bathias has investigated Udimet 500 nickel alloy (2) and found that the fatigue strength decreases by 200 MPa when moving from  $10^6$  to  $10^9$  number of load cycles, Fig. 5. In addition to this, the effect of testing frequency on fatigue results was found to be insignificant for this material.

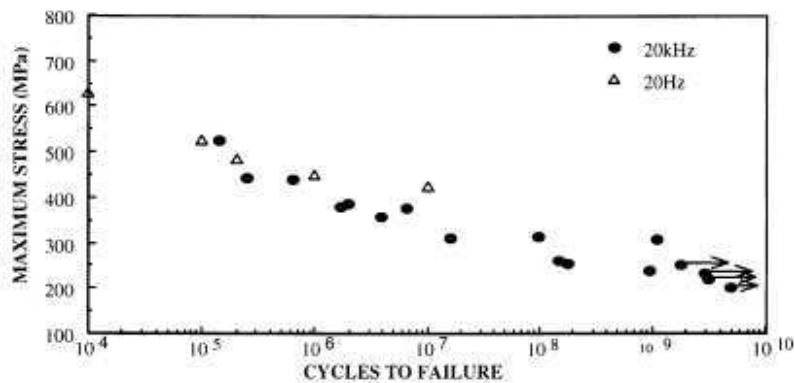


Figure 5. S-N curve for Udimet 500 alloy,  $R = -1$  (2).

Another example presents high temperature VHCF performance of N18 alloy used for manufacturing turbine disks (2). Some specimens have been purposely seeded with inclusions to monitor their effect in gigacycle domain. Testing was conducted at  $450^{\circ}\text{C}$  and two different load ratios:  $R = 0$  and  $R = 0.8$ , Fig. 6. As could be seen from the figure the seeded specimens generally had lower fatigue strength compared to unseeded, which underlines detrimental effect of inclusions on fatigue properties in the VHCF range.

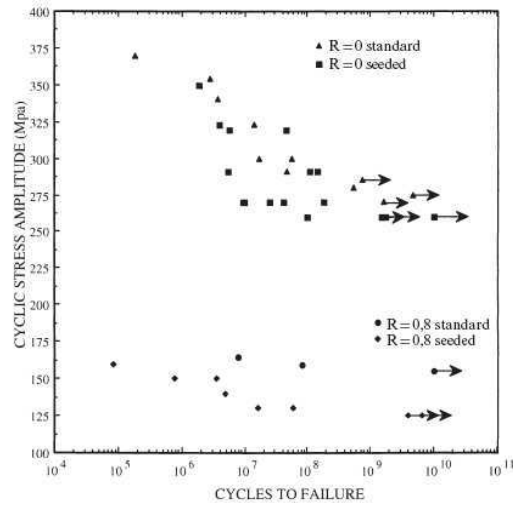


Figure 6. S-N curves for N18 nickel alloy at 450°C (2).

Q. Chen et al. investigated VHCF behaviour of nickel-based super-alloy Inconel 718 (3). Fatigue tests were carried out at ambient temperature with the load ratio  $R = -1$ . The results presented in Fig. 7 show that by decreasing stress amplitude a limit of 530 MPa was reached below which fatigue failure did not happen even at 10<sup>9</sup> cycles. However, it should be pointed out that some fatigue failure occurred beyond 10<sup>7</sup> load cycles. This indicates that the conventional definition of fatigue limit, such as stress level at which a material survives 10<sup>7</sup> cycles, is no longer applicable. During ultrasonic testing, fatigue cracks initiated from the slip bands irrespective of the stress level. In Fig. 7 VHCF fatigue results are supported by conventional testing of the same material at low frequencies, which give lower values of fatigue strength compared to high frequency testing.

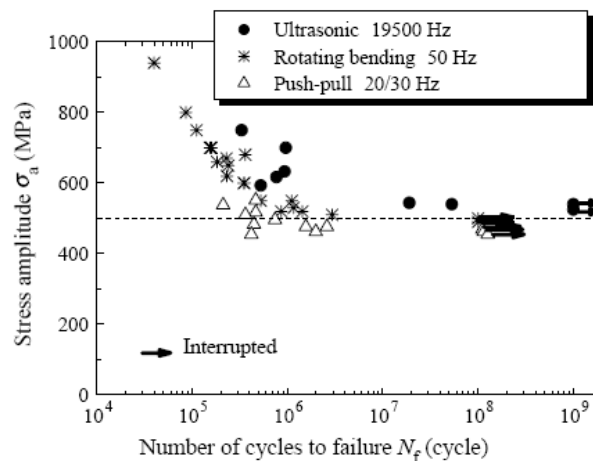


Figure 7. S-N curves for Inconel 718 nickel-based super-alloy (3).

### ***VHCF of aluminium alloys***

Aluminium alloys is another important category of materials used for manufacturing components subjected to VHCF. Following are some results obtained by ultrasonic testing on the common grades.

S. Stanzl-Tschegg and H. Mayer (4) investigated fatigue behaviour of 2024-T351 aluminium alloy tested at 20 kHz frequency under fully reversed loading conditions in ambient air and distilled water, Fig. 8. All the fatigue failures initiated at the surface of the specimens. As could be seen from the figure, the corrosive effect of distilled water reduced the fatigue strength by 30 - 40 %. This reduction had already been observed for cycles to failure as low as  $10^5$ , when the specimens' exposure to water was less than 1 min. Two specimens tested in water at 72 MPa did not break. Their surfaces were covered with grey aluminium oxide layer. It was difficult to judge if the observed endurance limit in water was the "intrinsic fatigue limit" or if this oxide layer prevented the surface from further oxidation attack.

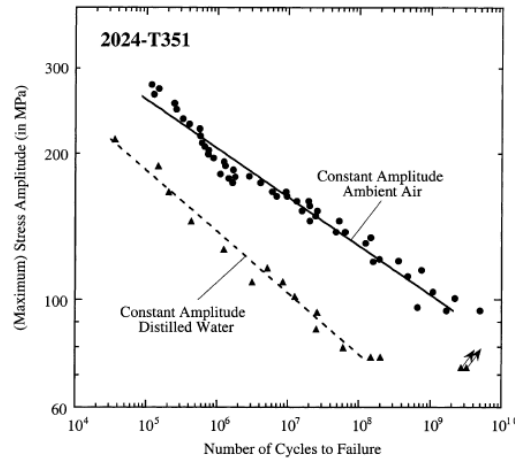


Figure 8. Fatigue data for 2024-T351 : dots – tested in air; circles – tested in ambient air. The lines refer to failure probability of 50%.

In (4) the fatigue results of two more aluminium alloys, namely an age hardened wrought alloy alloy of the 7xxx series and a particle reinforced alloy of the 6xxx series are presented. These alloys have been tested at both ultrasonic and conventional frequencies, Fig. 9. In this case no frequency effect has been observed. Tested materials did not show fatigue limit between  $10^5$  and  $10^9$  load cycles.

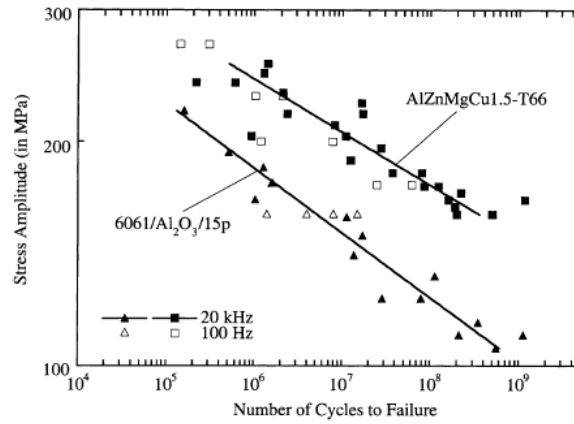


Figure 9. Fatigue data of AlZnMgCu1.5-T66 (squares) and 6061/Al<sub>2</sub>O<sub>3</sub>/15p (triangles), determined at 20 kHz (full symbols) and 100 Hz (open symbols) respectively. The lines refer to failure probability of 50 % in experiments at 20 kHz.

### *VHCF of magnesium alloys*

Energy savings from the use of weight-reducing components have attracted great interest in many industries. In this respect magnesium alloys have excellent properties: low density, high specific strength and stiffness, good machinability, etc. They can be used for production of structural parts, for example in engines, where fatigue life expectancy exceeds  $10^8$  load cycles. Therefore, the study of VHCF behaviour of magnesium alloys is necessary for their safe and reliable applications. F.Yang et al. (5) conducted 20kHz ultrasonic fatigue testing of AZ31 magnesium alloy at load ratio  $R=-1$ . The fatigue strength at  $10^9$  load cycles was calculated to be 89 MPa, Fig. 10. No fatigue limit was observed and the difference in fatigue strength between  $10^6$  and  $10^9$  load cycles was around 30 MPa, which is significant considering the low strength of the alloy. Fatigue failures mainly originated from the surface or slightly below the surface of the specimens. It was concluded that the main mechanism responsible for VHCF initiation in AZ31 alloy was cyclic deformation by twinning.

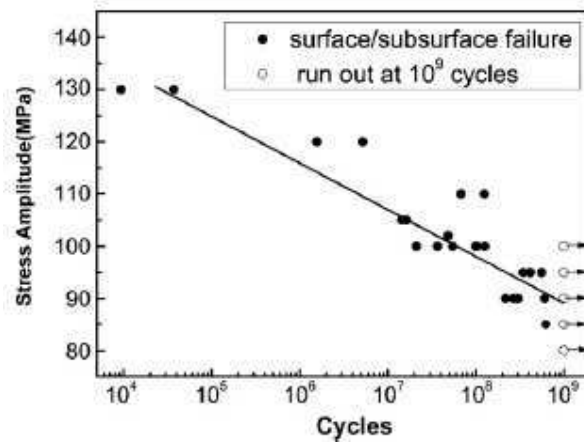


Figure 10. S-N curve for AZ31 magnesium alloy obtained by 20kHz ultrasonic testing at  $R=-1$ .

### ***VHCF of copper***

As a single-phase ductile metal copper is a typical representative of type I material. Pure copper does not have common defects for fatigue failure initiation in VHCF range, such as inclusions or porosity. With respect to fatigue in copper, it is believed that there is a certain threshold load amplitude above which persistent slip bands (PSBs) develop which then lead to shear band cracking and, finally, to failure. When the material is loaded at levels below this threshold, the PSBs would not be produced within the HCF range. However, a very gradual surface roughening would still be expected to develop, because the cyclic slip in the matrix structure of dislocations is not perfectly reversible, but has a small irreversible component (6).

In view of the above mentioned, it was suggested that in the VHCF regime, gradual surface roughening could eventually result in the formation of PSBs with the “ladder” structure, Fig. 11, and ultimately in shear band cracking. It is believed that at even lower stress amplitudes the irreversibility of slip becomes negligible, leading to a true fatigue limit.

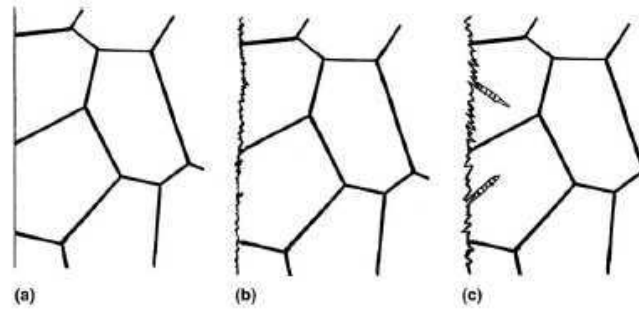


Figure 11. Schematic illustration of gradual surface roughening during fatigue loading below PSB threshold. a) initial surface; b) early surface roughening; c) later surface roughening. (6)

To verify these predictions the ultrasonic fatigue testing has been used. Stanzi-Tschegg et al. have tested polycrystalline copper specimen at stress amplitude ( $\sigma = 54$  MPa) distinctly lower than the PSBs formation threshold (7). This test was performed up to  $10^{10}$  load cycles, with regular interruptions to inspect the initially polished surface by means of atomic force microscopy (AFM). Even though the specimen did not fail at the end of the test, very pronounced surface markings in the form of slip band have become visible already after  $10^9$  cycles. This proves that cyclic slip in matrix dislocation structure is not fully reversible and the first stages of fatigue damage could be observed even at stresses below the PSB threshold.

In their recent work (8) on VHCF properties of polycrystalline copper, L. Kunz et al. conducted experiments for conventional grain (CG) size (around  $10\text{ }\mu\text{m}$ ) as well as ultra-fine grain (UFG) copper (grain size around  $300\text{ nm}$ ). In this way the dependence of fatigue life on grain size in VHCF regime could be analyzed. From Fig. 12 it could be concluded that the fatigue strength of UFG copper is approximately twice as high as that of CG copper in the whole range of fatigue lives from  $10^4$  to more than  $10^9$  load cycles. This increase in fatigue strength by the reduction of grain size is remarkable. It should be pointed out that these results refer to the commercial purity UFG copper. Whereas for high purity copper (99.99%) the

fatigue strength is lower but still significantly higher than for CG copper. This could be explained by the fact that high purity copper is rather unstable under cyclic loading (6).

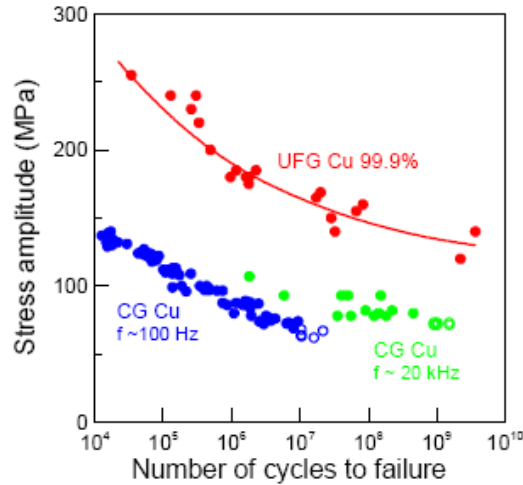
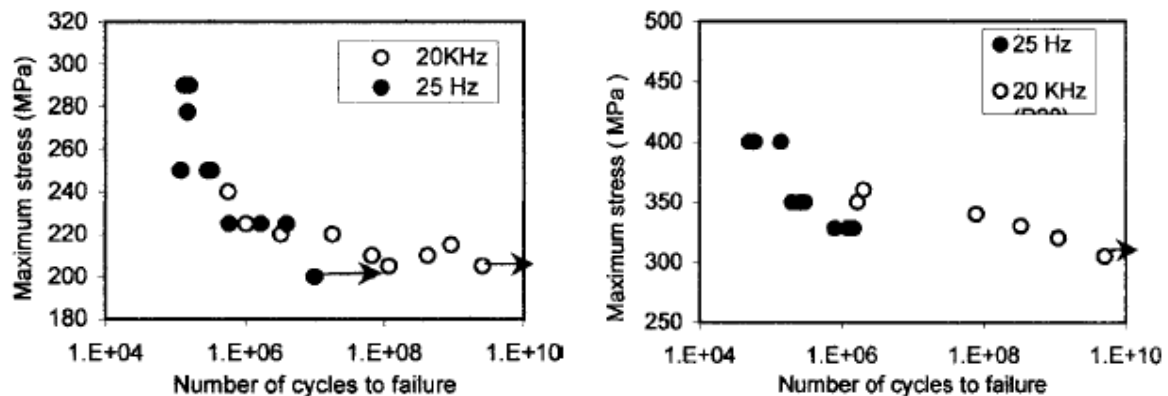


Figure 12. The comparison of S-N curves for CG and UFG copper. Full symbols represent failed, open symbols – survived specimens (8).

#### ***VHCF of spheroid graphite cast iron***

Good combination of tensile strength, wear resistance and ductility together with relatively low price, makes spheroid graphite (SF) cast iron the material of choice for many automotive structural applications. The required life expectancy for some components (suspension arms, gears, crankshafts, etc.) exceeds  $10^9$  load cycles. Q. Wang et al. conducted VHCF experiments coupled with traditional fatigue tests for this material (9). Two different load ratios  $R = -1$  and  $R = 0$  were used. The results, Fig.13, show that the specimens continue to fail beyond  $10^7$  cycles. In other word no fatigue limit was observed. The material exhibited two types of fatigue initiations: 1) from the surface; 2) interior initiation (dominant for more than  $10^7$  load cycles). The frequency effect was insignificant being more pronounced at  $R = 0$ .



(a)  $R=-1$

(b)  $R=0$

Figure 13. S-N curves for SG cast iron (9).

### ***VHCF of materials in brief***

As has been shown by experimental results presented above, the majority of the materials that are used for VHCF applications do not have a fatigue limit at  $10^9$  load cycles but instead exhibit continuous decrease in fatigue strength. The rate of this decrease varies from material to material and the factors influencing it are not well understood. However, it is clear that the lower fatigue strength at  $10^9$  compared to  $10^6$  load cycles should be accounted for in components subjected to VHCF. In other words, the conventional fatigue limit at around  $10^6$  load cycles is not a reliable concept.

One of the most important questions with respect to VHCF phenomena is what factors cause or contribute to fatigue failure. Fortunately, this question could be largely answered simply by careful observations and analyses of VHCF fracture surfaces. The origins of failures once again are different for various materials but they all have at least one thing in common – they all represent the weakest sites within a particular material with respect to fatigue process. In some materials these critical sites are micro-structural defects like inclusions, pores, etc. or even micro-structural inhomogeneities such as abnormal grains or platelets (common in titanium alloys). In addition to this, fatigue fracture could start at weak boundaries between phases or matrix and reinforcement particles as in composites.

In materials with high plasticity (ex. copper, aluminium alloys) surface roughening, formed as a result of cycle slip, often proves to be more detrimental with respect to VHCF than any available micro-structural discontinuities. Therefore, fatigue fracture originates from the surface even in very long life regime.

In view of the above mentioned it could be anticipated that the VHCF initiation sites in steels would be slag inclusions, pores or carbide segregations. VHCF behaviour of steels is the subject of discussion in the next section.

## **4. VHCF of steels**

The following is a brief overview of the VHCF results obtained from testing of different steels which are presently used for very long life applications. If not otherwise specified, the fatigue data presented below was comprised by “push-pull” testing of hour-glass specimens using ultrasonic equipment. The critical specimen sections were grinded and polished. Testing was performed in air using additional cooling in order to maintain the specimens’ temperature in the range of room temperature. Most experiments were conducted at load ratios  $R = -1$  or  $0.1$ .

For the sake of comparison the value  $\Delta\sigma_D$ , representing the difference in fatigue strength between  $10^6$  and  $10^9$  load cycles, is introduced.

### Low carbon sheet steel

Ultrasonic fatigue equipment enables also testing of specimens with the thickness less than 1mm (10). Low carbon ferritic steel was tested at load ratio  $R=-1$  and the results are presented in Fig. 14. The continuous decrease of fatigue strength with increasing number of cycles suggests that there is no fatigue limit for this material even though the difference of 25 MPa between fatigue strength at  $10^6$  and  $10^9$  load cycles is not significant.

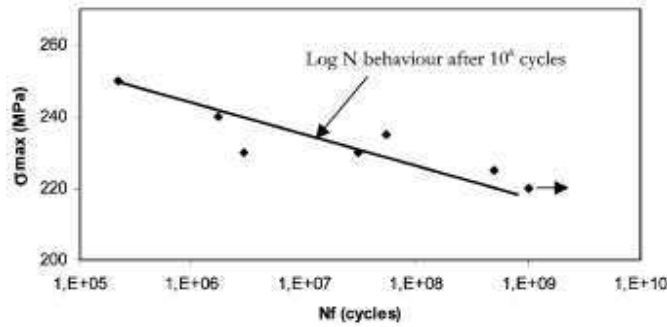


Figure 14. S-N curve for low carbon sheet steel.  $R = 0.1$ , 20 kHz;  $\Delta\sigma_D = 25$  MPa (10).

### Stainless steels

The significant decrease of 200 MPa in fatigue strength between  $10^6$  and  $10^9$  cycles is observed for 17-4PH martensitic stainless steel, Fig. 15 (10). While austenitic stainless steel 304 behave in a completely different manner (11) showing rather asymptotic fatigue strength evolution in VHCF regime, Fig. 16. For this material, even though some failures took place at about  $10^8$  load cycles, all fatigue cracks initiated from the surface. Another example is a 12% Cr martensitic stainless steel, Fig. 17. Here the difference  $\Delta\sigma_D = 40$  MPa is rather insignificant and the location of the crack initiations, similar to 17-4PH steel, is on the surface up to  $10^7$  cycles and from the interior at higher number of cycles.

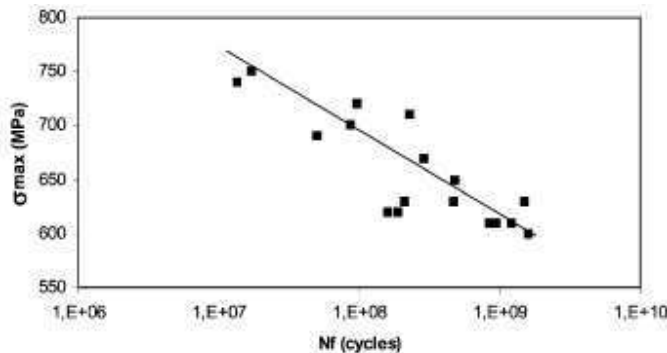


Figure 15. S-N curve for 17-4PH martensitic stainless steel.  $R = -1$ ; 20 kHz;  $\Delta\sigma_D = 200$  MPa (10).

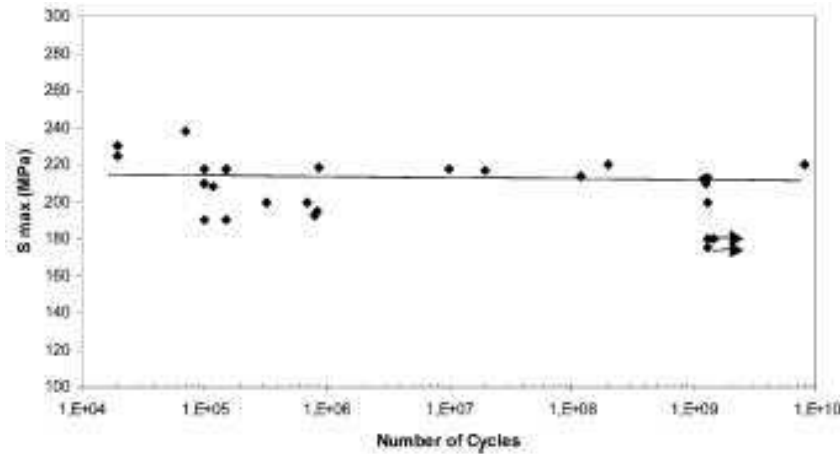


Figure 16. S-N curve for 304 stainless steel.  $R = -1$ ; 20 kHz (11).

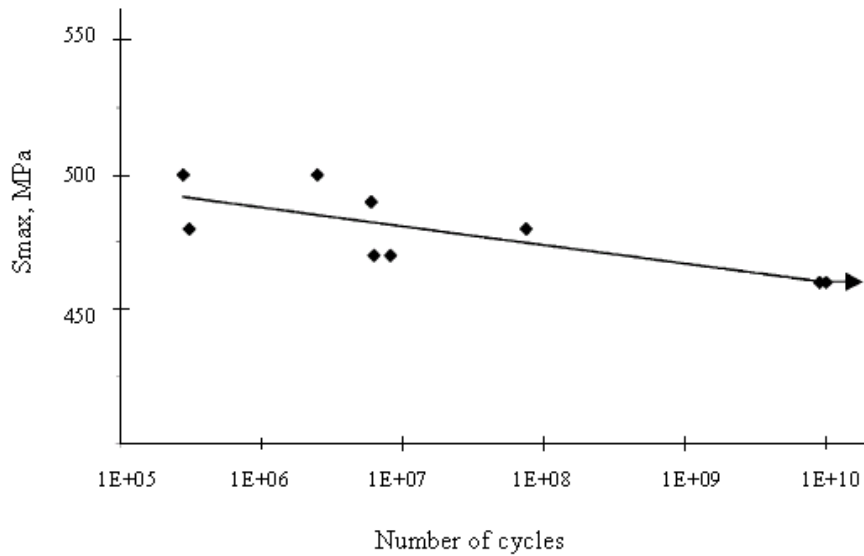


Figure 17. S-N curve for 12% Cr stainless steel.  $R = -1$ ; 20 kHz;  $\Delta\sigma_D = 40$  MPa (11).

### Spring steels

Q. Y. Wang et al. investigated in (12) two types of ultra-high strength spring steel wires that are widely used in automotive sector: a Cr-V steel of valve spring quality (VSQ, ASTM A232) and a Cr-Si steel VSQ wire (ASTM A877). The results of ultrasonic fatigue testing at 20 kHz with load ratio  $R = -1$  are shown in Fig. 18. It seems that Cr-V steel does not deteriorate in terms of fatigue strength when tested in VHCF range. Whereas Cr-Si steel shows a significant decrease ( $\Delta\sigma_D = 170$  MPa) in fatigue strength between  $10^6$  and  $10^9$  load cycles. Fatigue crack initiations were observed at internal defects when number of cycles was higher than  $10^7$ . At lower lives the initiation started from the surface.

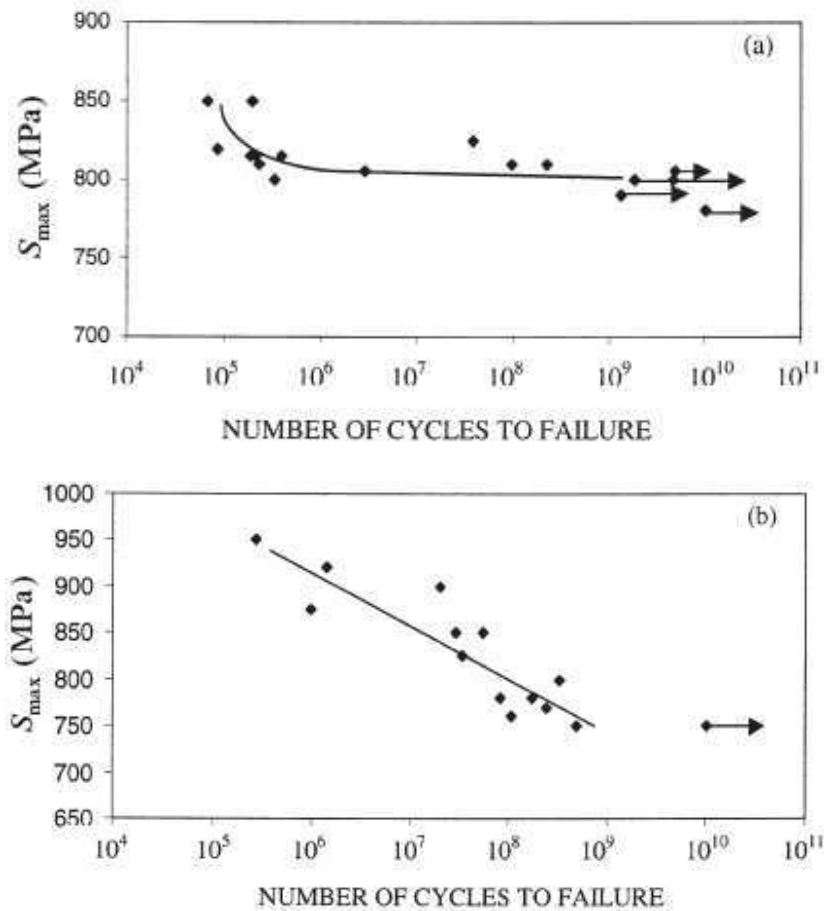


Figure 18. S-N curves at  $R = -1$ , 20 kHz: (a) Cr-V spring steel; (b) Cr-Si spring steel,  $\Delta\sigma_D = 170$  MPa (12).

### ***Cold work tool steel***

In (13) C. Sohar et al. investigated the VHCF behaviour of AISI D2 steel, which is a medium carbon, high chromium cold work tool steel. It contains numerous primary carbides, required for high abrasion resistance and hardness. However, with respect to fatigue those are the primary crack initiating sites. The service life of a tool produced from this material depends both on its abrasion resistance and fatigue performance. In this work the authors tested two series of specimens: K110L-I and K110L-I with high and low surface residual stresses (RS) respectively. The results of ultrasonic testing at 20 kHz with load ratio  $R = -1$  are presented in Fig. 19.

The fatigue crack initiation sites were carbides and carbide clusters, located in the interior as well as in the surface layer. Primary carbides were found to have fractured at the entire fracture surface. What is particularly astonishing is a dramatic decrease by around 300 MPa in fatigue between  $10^6$  and  $10^9$  cycles.

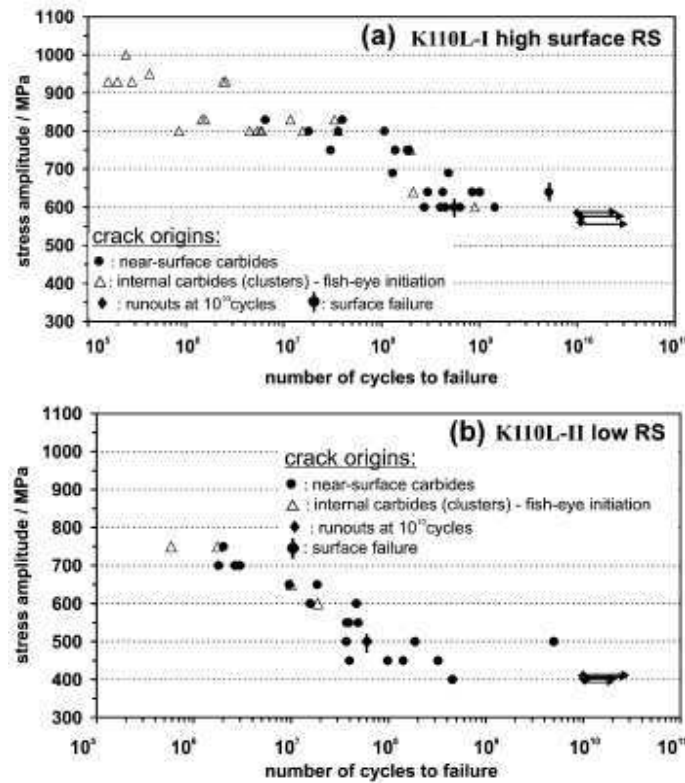


Figure 19. S-N curve for AISI D2 steel: (a) high RS on the surface; (b) low RS on the surface. 20 kHz;  $R = -1$ ;  $\Delta\sigma_D = 300$  MPa. (13)

### Bearing steel

T. Sakai et al. (14) have extensively evaluated VHCF properties of high-carbon-chromium bearing steel JIS:SUI2, whose chemical composition is shown in Table 2. The specimens have been fatigue tested in push-pull axial loading (load ratio  $R = -1$ ) using servo-hydraulic testing machine at frequency of 50 Hz. Specimens heat treatment was carried out as follows: quenched – 1108K/40min + Oil cooling; tempered – 453K/120min + air cooling.

Table 2  
Chemical composition of JIS:SUI2

C	Si	Mn	P	S	Cr	Cu	Ni	Mo	O
1.01	0.23	0.36	0.012	0.007	1.45	0.06	0.04	0.02	8ppm

The fatigue results are presented in Fig. 20 a). For the sake of comparison the S-N curve, obtained by fatigue testing of the same material in rotating bending, is shown in Fig. 20 b). The SEM observations showed that there were two types of fatigue failures: 1) from the surface; 2)

“fish-eye” interior fracture from an inclusion. The second type could be further divided on specimens with the “fish-eye” reaching surface and those where the “fish-eye” is inside the material.

If the same stress is applied to specimens in these respective loading types, the maximum stressed region will be located close to the surface in rotating bending specimens, while in axial loading the maximum stressed area is more or less the whole cross-section of a specimen. In other words tested volume is larger in axial loading, which gives a higher probability of finding a critical defect, which would initiate fatigue fracture. This explains why fatigue strength is higher for rotating bending experiments.

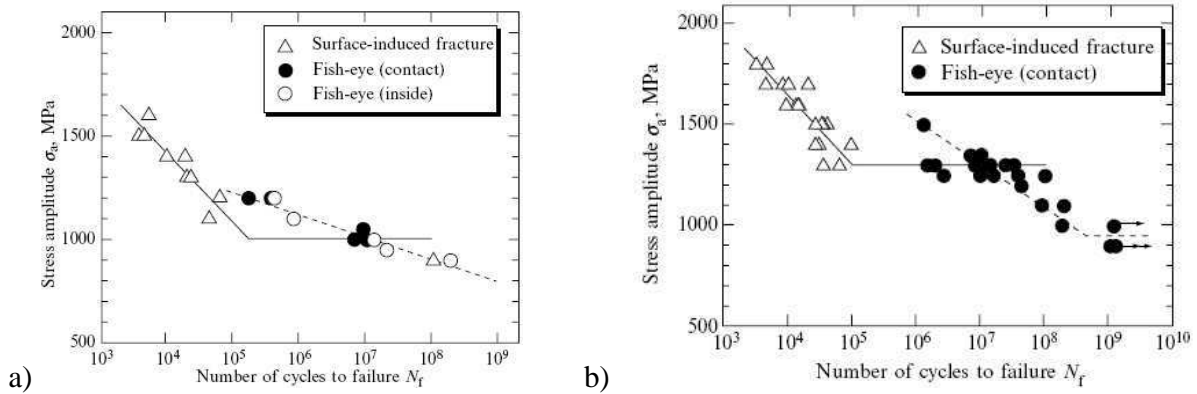


Figure 20. S-N curves for JIS:SUJ2 bearing steel: a) axial loading; b) rotating bending (14).

From the fatigue results presented in Fig. 20 it could be concluded that tested material does not have a fatigue limit at very long lives. Two fracture modes (initiation from the surface and “fish-eye” interior initiation) have been identified, with more clear separation between them found for rotating bending tests. Finally, all the “fish-eye” fractures initiated from inclusions.

### ***Rail steel***

Another important material for technical applications in which components are subjected to VHCF is Rail Steel 700. Its fatigue properties have been evaluated by C. Bathias et al. in (11). The results presented in Fig. 21 indicated that the material does not have a fatigue limit in very long life regime. The difference in fatigue strength between  $10^6$  and  $10^9$  load cycles constitute 70 MPa.

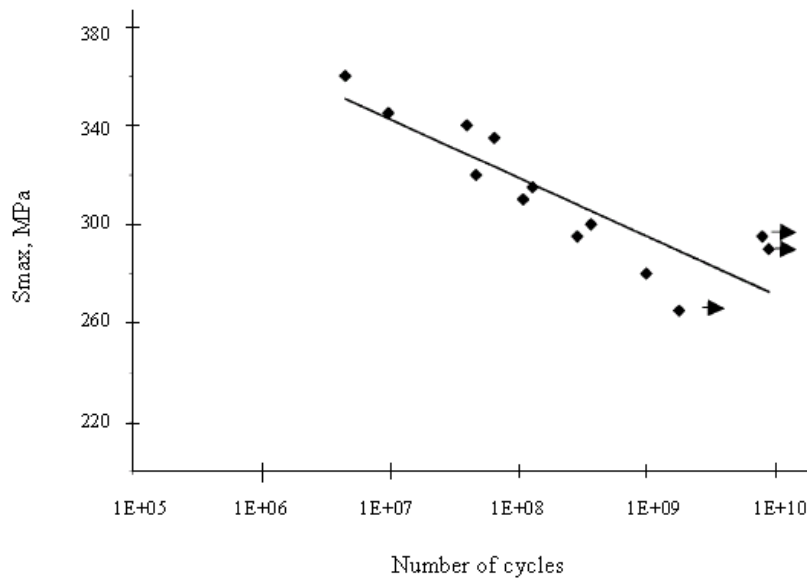


Figure 21. S-N curve for rail 700 steel.  $R = -1$ , 20 kHz,  $\Delta\sigma_D = 70$  MPa (11).

### ***VHCF of steels in brief***

The presented review of VHCF behaviour of various steels indicates that in most cases the fatigue limit is non-existent concept. Instead, the majority of materials show continuous degradation of fatigue strength with increasing number of load cycles. With respect to difference in fatigue strength between  $10^6$  and  $10^9$  load cycles, materials could be divided into type 1 and type 2 materials for which this difference is less than 50 MPa and more than 50 MPa respectively. Among the representatives of type 1 materials are low-carbon steels, stainless steel 304, 12% Cr steel and spheroid graphite cast iron. For type 2 material the difference reaches 300 MPa, which means higher slope of S-N curve and, most importantly, this decrease in fatigue strength should be accounted for when producing components subjected to VHCF.

From the fatigue experiments on ferrous materials an important difference between LCF and VHCF is observed with respect to crack initiation. In LCF regime crack initiation is a product of progressive surface roughening, which is a result of plastic deformation. However, in VHCF the crack initiates from the interior rather than the surface. This could be explained by the fact that in this case the stresses are too low to produce plastic deformation in the form of surface roughening, and the internal defects such as inclusion, pores, etc. become the main source for crack initiation.

In general, it is rather difficult if not impossible at present to predict VHCF behaviour of a material without experimental testing. In line with growing variety of materials that are used in VHCF applications under various conditions (temperature, environment, stress state, etc.), the interest for extensive evaluation of VHCF properties is also steadily increasing. Ultrasonic testing is so far the only practical means to investigate fatigue behaviour for very long lives, which implies further development and diversification of this technique.

## 5. VHCF crack initiation and growth

### *Duplex S-N curve*

In light of the present knowledge about VHCF of materials the conventional S – N curve with the asymptotic fatigue limit could be modified into the ones shown in Fig. 21 (15), which are often referred to as duplex or multi-stage S – N curves. The slight difference between the curves, Fig. 22 a) and b), reflects two viewpoints as to whether the fatigue limit in the VHCF range exists, Fig. 22 a), or not, Fig. 22 b). The distinction is made between surface and internal failures. Broad experimental evidence suggest that in the absence of the stress raises on the surface, with increasing number of cycles there is a gradual shift from fatigue failures initiating from the surface towards those starting at the internal material defects and leading to the development of the so-called “fish-eye” on the fracture surfaces. This situation can occur at relatively low stresses, when cyclic slip at the surface does not give rise to sufficient surface roughening.

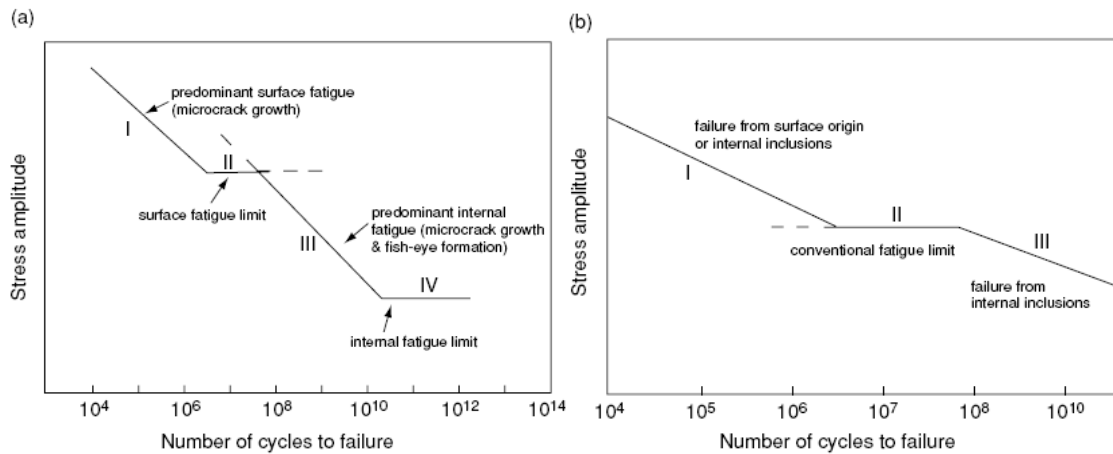


Figure 22. Schematic illustration of duplex S-N curve with (a) and without (b) fatigue limit in VHCF range. I – LCF; II – HCF; III and IV – VHCF (15).

### *Stages in VHCF*

Fatigue failure process in the very long life regime could be divided into following stages: 1) crack initiation (usually from internal material defect); 2) crack growth within the “fish-eye”; 3) crack growth outside the “fish-eye”; 4) rapid fracture. The above stages are identified on the typical VHCF fracture surface that is presented in Fig. 23. The “fish-eye” is a characteristic feature of the VHCF failure and could be defined as circular area (usually 0.5 – 1 mm in diameter) that surrounds failure origin site, and was formed as a result of internal circular crack propagation.

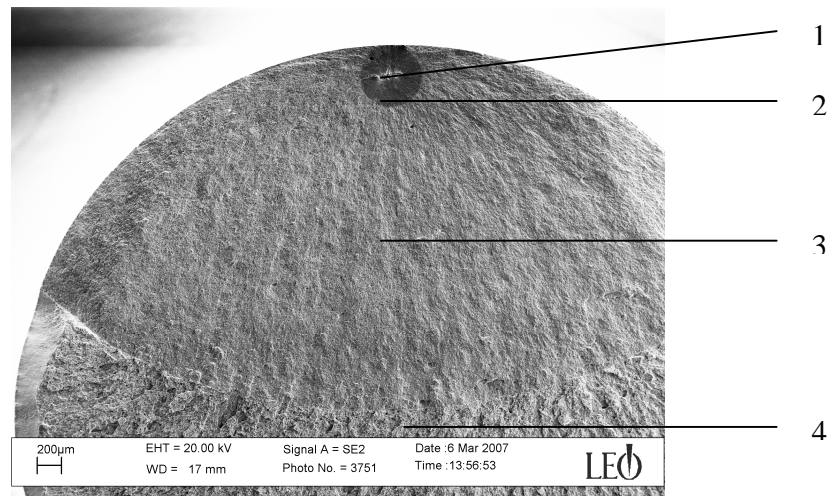


Figure 23. Typical VHCF fracture surface obtained in a specimen made of AISI H13 steel.

It is very important to be able to understand and predict fatigue life in terms of crack initiation and small crack propagation. Generally excepted view is that at high stresses fatigue life is mainly determined by crack growth, while at low stresses components' life is primarily consumed by the process of crack initiation. A number of researches have demonstrated that a portion of life attributed to crack nucleation is above 90% in the high cycle regime ( $10^6 - 10^7$ ) for steels, titanium, aluminium and nickel alloys (1). This fraction is even higher when it refers to the VHCF regime. In one study Billaudeau and Nagot (16) analysed the role of environment in particular with respect to crack growth, and concluded that the VHCF crack initiation governs fatigue life both for surface and internal defects. In another work (17) Paris et al. showed that the number of cycles required for failure by crack propagation can only be a small fraction of total fatigue life.

Therefore, in order to predict and improve the VHCF performance of various materials it is required to obtain a comprehensive knowledge as to what is the cause or causes for initiation of fatigue fracture in super-long life regime for a particular material under certain conditions. Then the question is how these causes could be eliminated or at least their deteriorating effects be reduced in a predictable way so as to secure reliable and long-lasting service of the components subjected to VHCF.

### ***Origins of VHCF failures***

Generally, but not always, in VHCF the cracks initiate from material defects such as inclusions (high strength steels, martensitic stainless steels, bearing steels, spring steels, etc.) or pores (mainly PM materials). However, sometimes the initiation is attributed to micro-structural anomalies like abnormal grains, long platelets or perlite colonies, etc. For example, it is well known that there are no inclusions or porosity in titanium alloys. Therefore, the crack initiates from metallurgical discontinuities such as platelets found in primary alpha phase (1). In some materials the main source for VHCF failure initiation could be large carbides or carbide clusters (cast irons and some steels).

It is thought that at small loads, the stress concentration due to metallurgical microstructure misfit becomes an important factor for fatigue initiation. The above mentioned sites serve as efficient stress concentrators. The fact that the probability of finding these defects or anomalies in the bulk is greater than on the surface, could be an explanation as to why most VHCF failures are internal.

VHCF failures starting from the surface are also common for some materials (mainly for pure metals, for instance – copper). Here the development of persistent slip bands on the surface, eventually lead to cracking and failure (6). Another special case is Al-Si cast alloys, in which the VHCF initiation begins at the surface. This behaviour could be explained by high density of pores always present on the specimen surface.

## 6. VHCF models

### *Murakami model*

Y. Murakami et al. in their multiple works (18-25) studied different factors affecting fatigue process in ultra-long life regime. They particularly emphasize the crucial role that the hydrogen trapped by non-metallic inclusion plays in initiating fatigue failure. The summary of their findings is presented below.

According to the authors, for many steels at careful observation of the “fish-eye” mark in optical microscope, a dark area could be found on the fracture surface in the vicinity of the inclusion, Fig. 24. It was named an optically dark area (ODA). Murakami et al. suggest that its formation is influenced by hydrogen trapped around the fatigue initiating inclusion, Fig. 25. Based on the detailed observations, ODA growth is not due to the ordinary cycle by cycle fatigue process, but instead is governed by a very slow mechanism that incorporates synergistic effect of cyclic stress and the trapped hydrogen. According to scanning electron microscopy observations, ODA has a very rough morphology compared to the remaining area of the “fish-eye”.

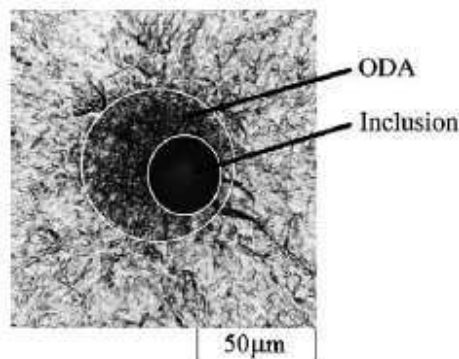


Figure 24. Optical micrograph of the fracture origin (JIS SCM435,  $\sigma = 561$  MPa,  $N_f = 1.11 \times 10^8$ ).  
ODA - optically dark area around the inclusion. (26)

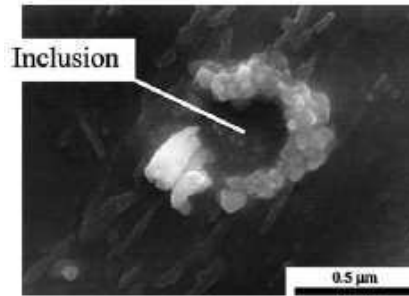


Figure 25. Hydrogen trapped around a non-metallic inclusion ( $\text{Al}_2\text{O}_3$ ) observed by tritium autoradiography (26)

Murakami et al. show that fatigue crack growth without the assistance of hydrogen starts after the fracture area parameter  $\sqrt{\text{area}}$ , Fig. 26, exceeds the critical value  $\sqrt{\text{area}_c}$ , which incorporates the area of non-metallic inclusion as well as the ODA area where fatigue crack propagation is aided by hydrogen. It could be calculated from:

$$\sqrt{\text{area}_c} = [1.56(HV + 120)/\sigma]^6, \quad \text{where } \sigma - \text{stress amplitude.}$$

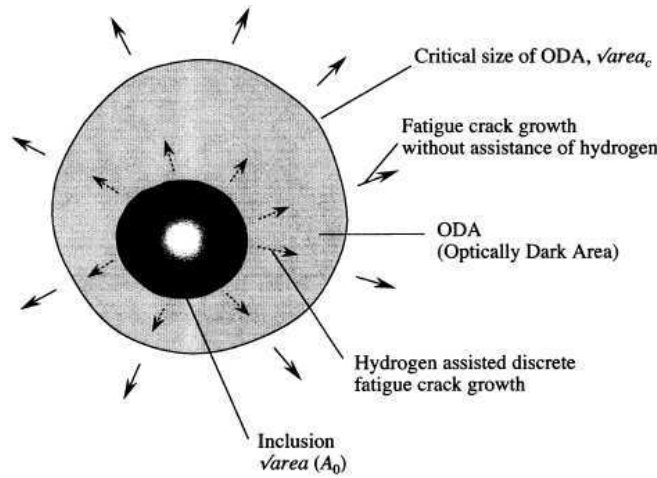


Figure 26. Schematic illustration of fatigue crack growth from non-metallic inclusion in the VHCF range (21).

It is hypothesized that the reason for fatigue failure in the super-long life regime (over  $10^7$ ) is that the mechanical fatigue threshold for a small crack emanating from a non-metallic inclusion is reduced by an environmental effect associated with hydrogen trapped at the inclusion. Accordingly, it is presumed that when the size of ODA exceeds the critical size defined by the intrinsic material fatigue limit, the fatigue crack grows without the assistance of hydrogen, Fig. 27. Although the combined mechanism of cyclic stress and hydrogen is not clear, the possible effect may be related to enhancing the mobility of screw and edge dislocations and reducing internal friction by hydrogen.

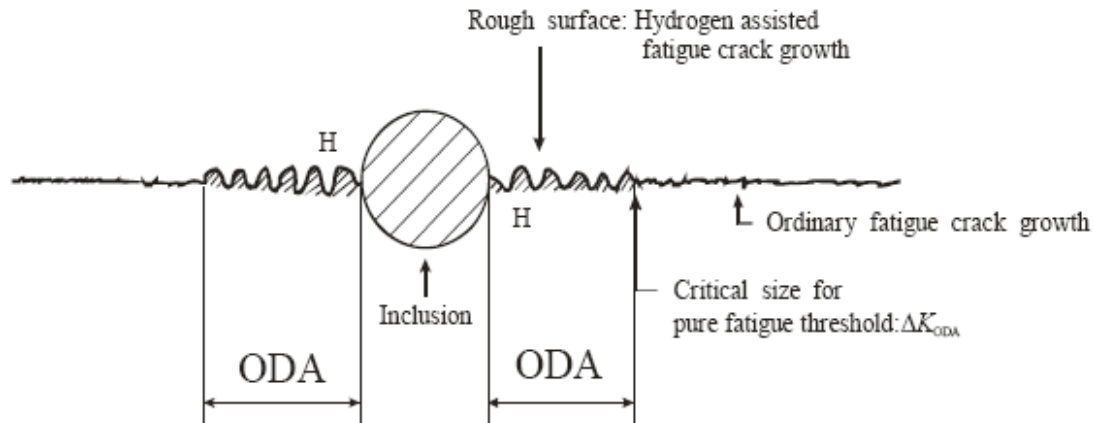


Figure 27. Scheme of hydrogen-assisted fatigue fracture in ultra-long life regime (27).

In one study (22) three series of specimens, with various hydrogen content were fatigue tested and analyzed. It was found that the size of the ODA area increased when raising hydrogen content. In addition to this, the ODA could not be observed on the fracture surfaces of specimens failed at small number of cycles ( $10^5$ ), while the relative size of ODA to the original inclusion size increases with increase in fatigue life.

In another work (21) Murakami et al. calculated the number of cycles required for the crack to grow from the ODA border to the “fish-eye” border in the Cr-Mo steel SCM435. They found that it ranges from  $10^5$  to  $10^6$  cycles, which is but a small fraction of the total fatigue life in the VHCF range where ODA is formed. This result indicates that the VHCF life is mostly consumed in crack initiation and growth within the ODA.

Thus the influence of hydrogen is of great importance for fatigue failure in the VHCF regime. It is known that heat treated steels tend to contain a high hydrogen content around inclusions. Therefore, this particular problem deserves additional attention when designing high strength steel components subjected to VHCF.

### ***Carbide de-cohesion model***

K. Shiozawa et al. conducted a study of subsurface crack initiation and propagation mechanisms in specimens made from high carbon chromium bearing steel and subjected to VHCF (28). A white-bright facet area was found in the vicinity of the fracture origin when observed by SEM. It had a very rough and granular morphology in comparison with the remaining area inside the “fish-eye”. The area was called “granular bright facet” (GBF). Later experiments verified that the size of GBF is the same as observed by Murakami ODA.

This model describes the mechanisms of GBF formation. Their understanding is of great importance as it is during this stage that the largest portion of fatigue life is consumed. Detailed analysis of the morphology in the GBF area was carried out using a scanning probe microscope

(SPM) and a scanning electron microscope (SEM). The simulation of fatigue fracture process was made using fracture surface topographic analysis (FRASTA) method proposed by Kobayashi and Shockey. FRASTA is a computational procedure for reconstruction the process of crack growth on a microscopic scale by comparing topographic features of opposing fracture surfaces. This technique allows for examination of sub-surface crack growth as it is difficult to directly observe cracks inside a specimen.

In addition to this, the fracture surface roughness was measured and found that the roughness of GBF area is about 2.5 times greater than that outside the GBF area. Supposing that some roughness on the fracture surface was formed by the remaining carbide particles and the pits left by the ones that had been pilled off, a high density of carbon should be detectable in the GBF area. This was confirmed by electron probe microanalysis (EPMA).

Based on: 1) thorough observations of fracture surfaces with SEM and SPM, 2) measurements of roughness, 3) the FRASTA computational simulation of the crack formation, 4) carbon distribution by EPMA, K. Shikozawa et al. proposed the following model of GBF formation:

At the very beginning of the fatigue process multiple micro-cracks are initiated by decohesion of spherical carbides from the matrix in the vicinity of the non-metallic inclusion, Fig. 28a). During fatigue process these micro-cracks grow and eventually coalesce with each other forming GBF area, Fig. 28b). The micro-cracks propagate along the boundaries between the matrix and the carbides. Therefore, the roughness generated at the fracture surface corresponds to the carbides size. At this stage the rate of micro-crack propagation is very low. However, having grown to a certain size the crack marks the end of the GBF area and continues to propagate as an ordinary crack with little dependence on the microstructure forming the remainder of the “fish-eye”, Fig. 28c). It could be concluded that the greater roughness of the fracture surface in the GBF zone compared with the surrounding area is formed by the holes from which the carbides have been peeled off and by the carbides themselves that stick out from the matrix. The roughness outside the GBF area is small because the fatigue crack propagates in a way shown in Fig. 28d).

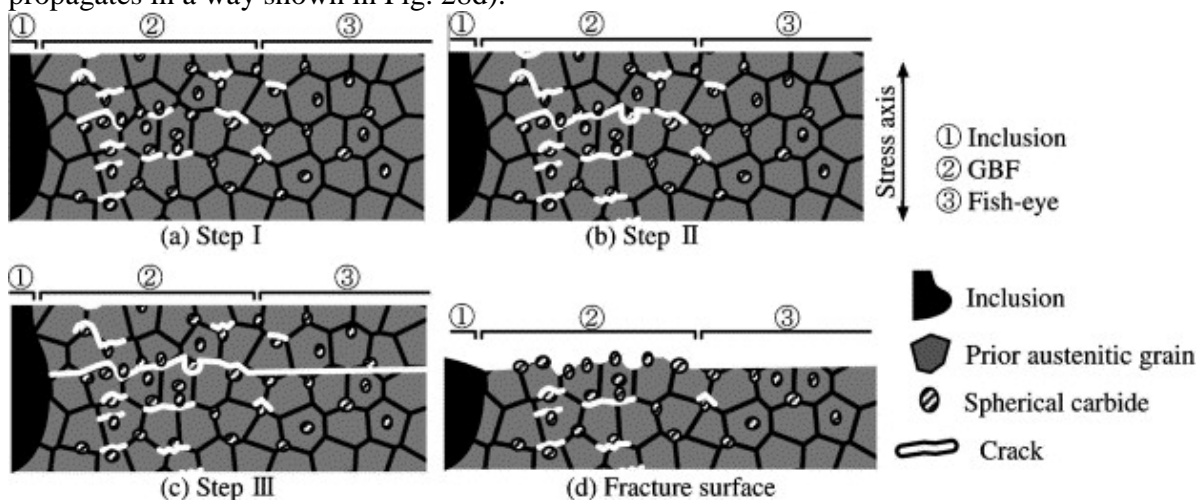


Figure 28. Proposed model for the formation of GBF area around an inclusion during VHCF (28).

The above model named “dispersive de-cohesion of spherical carbides” describes the development of the GBF area in the vicinity of non-metallic inclusion during VHCF, which subsequently leads to the crack formation that results in fatigue fracture. On the other hand, at high stress levels and small number of load cycles a fatigue crack occurs at an inclusion due to stress concentration without the formation of the GBF zone. The models validity was confirmed by authors (29) through an experimental study using high speed tool steel.

### *Fatigue predicting model based on single particles as well as clusters*

In (30) the model that predicts fatigue strength from the particles size distribution data is described. It is based on fracture mechanics and the model assumes that a specimen would fail if it contains at least one carbide or inclusion of a critical size. Another assumption that is made here is the existence of cracks at the particles even prior to fatigue testing, Fig. 29. The critical particle/crack size is reached if the stress intensity  $\Delta K_I$  of the crack is above the threshold value for crack propagation  $\Delta K_{th}$  (the value of 4 MPa was used as the input data for the model). The model only considers cracks around single particles.

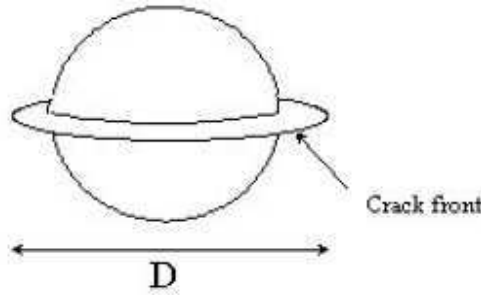


Figure 29. Diameter of a crack initiated at an internal carbide particle or inclusion (30).

By measuring the particles size, the conditions for crack propagations could be described by the stress intensity formula using linear elastic fracture mechanics:

$$\Delta K_I = 2 \cdot \Delta \sigma \cdot \sqrt{\frac{D}{2\pi}}$$

Thus, the critical size of such a particle versus the applied stress will become:

$$D(\Delta \sigma) = 2\pi \cdot \left( \frac{\Delta K_{th}}{2 \cdot \Delta \sigma} \right)^2$$

By rewriting the above equations, the stress range which would be the calculated fatigue strength based on the particles' size distribution  $D$  becomes:

$$\Delta \sigma = \frac{\Delta K_{th}}{2 \sqrt{\frac{D}{2\pi}}}$$

Therefore, if the particle distribution is known it would be possible to integrate over the geometry of the specimen and calculate the probability of finding at least one particle which has  $\Delta K_I > \Delta K_{th}$  within the load effected volume.

The experimental findings have demonstrated that a fatigue crack can initiate from a cluster of carbide particles. A cluster is defined as a spherical volume of material where the local carbide fraction is above a certain threshold level. The model assumes that a cluster of carbides can cause a fatigue crack of the same size as the cluster itself, Fig. 30. The possibility of locally raised carbide fraction above the threshold value is predicted by the model.

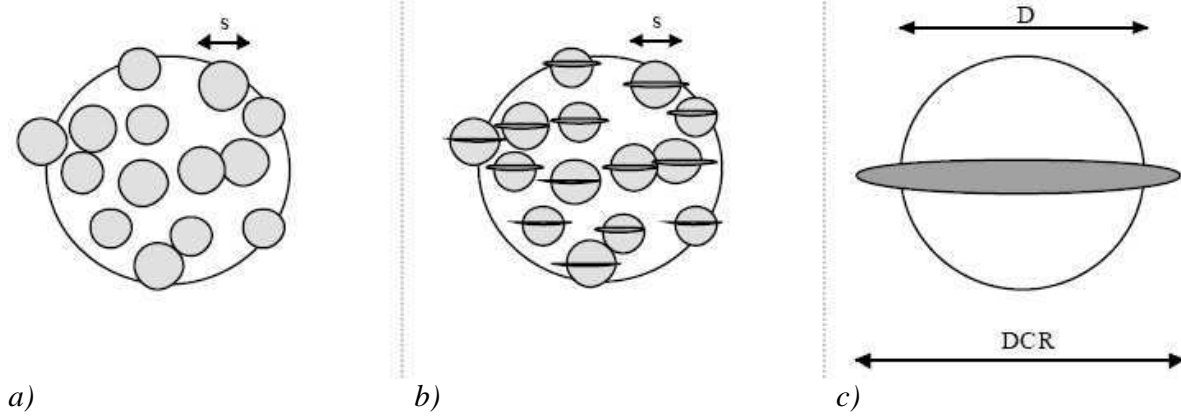


Figure 30. a) cluster of carbides; b) cracks at carbides in clusters; c) crack through cluster (30).

The fatigue predicting model both based on single particles or clusters are thoroughly presented with examples of applications in (30).

### ***P.Paris' fracture mechanics calculations***

It is shown in (31) that in VHCF regime the crack growth constitutes insignificant portion of the total fatigue life. Instead, the importance of fatigue crack initiation stage has been repeatedly emphasized. P. Paris at al. in his paper (17) divides the total “fish-eye” fatigue life into three stages: 1) crack initiation; 2) crack growth from small to long; and 3) crack growth from long to a critical size.

Fig. 31 presents a diagram with relative fatigue crack behaviour, where small crack starts from a defect of size  $a_0$  and becomes long at  $a_i$ . The crack growth rate is considered to be higher for small cracks then for long ones at the same nominal driving force due to lack of crack closure. The transition point from small to long cracks is located at a factor  $X$  from the threshold corner on the stress intensity axis.  $X$  is maximum for low load ratios ( $R=0$ ,  $X=3$ ) and minimum for high load ratios ( $R>0.8$ ,  $X=1$ ).

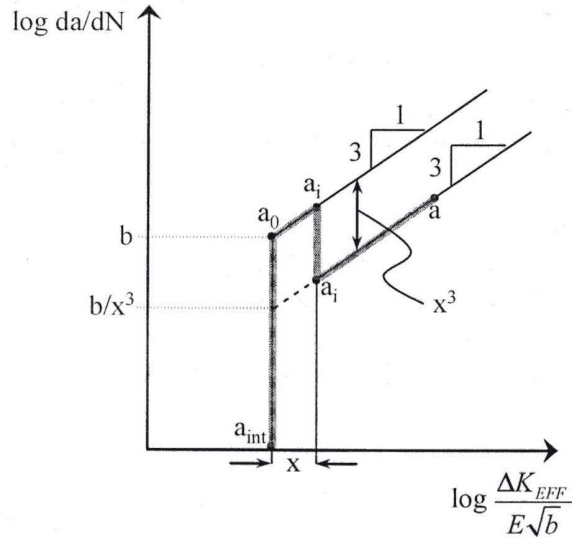


Figure 31. Fatigue crack growth for small (from  $a$  to  $a_i$ ) to long (from  $a_i$  to  $a$ ) cracks.

The total fatigue life  $N$  could be estimated from:

$$N = N_{\text{int}} + N_{a_0 \rightarrow a_i} + N_{a_i \rightarrow a}$$

By integrating crack growth law

$$\frac{da}{dN} = b \left( \frac{\Delta K_{\text{eff}}}{E\sqrt{b}} \right)^3$$

and using stress intensity formula for internal circular cracks

$$\Delta K = \frac{2}{\pi} \Delta \sigma \sqrt{\pi a}$$

P. Paris et al. established the following expressions for calculating fatigue life of small cracks, from  $a_0$  to  $a_i$ :

$$N_{a_0 \rightarrow a_i} = \frac{\pi E^2}{2(\Delta \sigma)^2} \left[ 1 - \sqrt{\frac{a_0}{a_i}} \right]$$

and respectively fatigue life of long cracks, from  $a_i$  to  $a$ :

$$N_{a_i \rightarrow a} = \frac{\pi E^2}{2(\Delta \sigma)^2} \left[ x^3 \sqrt{\frac{a_0}{a_i}} - x^3 \sqrt{\frac{a_0}{a}} \right]$$

The experimental results for different steels have shown that in the VHCF the fatigue life portion that corresponds to the crack growing from  $a_0$  to  $a$  constitute only insignificant part (less than 1%) of the total fatigue life  $N$ . This statement is valid even under various load ratios  $R$  and with the diverse range of transition sizes from small to large cracks.

## Concluding remarks

The use of ultrasonic fatigue testing equipment is at present the only viable alternative for the investigation of the VHCF properties of materials. As discussed earlier, it allows the application of different types of loading at various temperatures and with possibility of choosing the environment.

It is a general view that in VHCF regime the crack initiation and not propagation stage is the life-controlling and consumes close to 99 % of the total number of load cycles to failure. This emphasises the importance of recognising the crack origins and understanding the mechanisms of crack initiation and conditions under which they operate. Depending on the material possible initiation sites could be inclusions, pores, interfacial boundaries, abnormal grains, platelets, persistent slip bands, etc. With respect to steels, the most common fatigue crack origins in the VHCF regime are slag inclusions, pores (mainly in powder metallurgy produced steels) and large carbides or their segregation sites.

Regarding the mechanisms of VHCF crack initiation in steels, one of the most supported views is the “hydrogen assisted crack growth” proposed by Murakami. Hydrogen, often trapped at slag inclusions as well as in pores, lowers the effective stress intensity threshold required for a crack to propagate. For steels with high volume fraction of carbides the “carbide de-cohesion model” developed by Shiozawa et al. is a plausible explanation of how a fatigue crack is created. Assuming that during initiation the crack increases in size with each load cycle by as small length as one inter-atomic distance, the crack formation and growth stage would still be only a small fraction of a total VHCF life. This raises a question about the existence of “nothing happening” load cycles either prior to crack initiation or during initiation stage, which represent the major part of total fatigue life. Such reasoning formulates another question, which to the author’s knowledge did not found much attention in literature, that is when and under what circumstances the “nothing happening” load cycles become destructive to the material.

Unfortunately, the absence of hydrogen would not eliminate the VHCF phenomenon in steels, which shows that hydrogen is just one of the many factors that influence the fatigue strength of steels in giga-cycle regime. Among others are the defects’ (inclusions, pores, etc.) size, shape, type, distribution, density, position with respect to acting stresses, etc. Defect type, for example, can influence the stress state in the surrounding matrix, its cohesion to it, etc. Temperature, environment and matrix microstructure are additional factors that have a significant effect on fatigue process.

Obviously, for different types of steels, or materials in general, the controlling factors would be different. Therefore, considering the range of VHCF influencing parameters and their varying importance, it is unfeasible to develop a general VHCF model for all steels or even smaller domain such as tool steels. Which is why, the only practical way to study VHCF behaviour of materials is to experimentally test them individually. Based on the results, the conclusions should be drawn as to how the fatigue strength of a particular material could be improved. The experimental data in the literature is still rather scarce and even the available one would benefit from further verification. The VHCF performance of tool steels, which could be used for very long life applications, is one of the areas requiring further research.

## References

- (1) Bathias C, Paris PC. Gigacycle fatigue in mechanical practice. NY 10016, USA: Marcel Dekker; 2005.
- (2) Bathias C. There is no infinite fatigue life in metallic materials. *Fatigue & Fracture of Engineering Materials & Structures* 1999 07;22(7):559-65.
- (3) Chen Q, et. al. Small crack behavior and fracture of nickel-based superalloy under ultrasonic fatigue. *Int.J.Fatigue* 2005 10;27(10):1227-32.
- (4) Stanzl-Tschegg SE, Mayer H. Fatigue and fatigue crack growth of aluminium alloys at very high numbers of cycles. *Int.J.Fatigue* 2001;23:231-237.
- (5) Yang F, Yin SM, Li SX, Zhang ZF. Crack initiation mechanism of extruded AZ31 magnesium alloy in the very high cycle fatigue regime. *Materials Science and Engineering: A, Structural Materials: Properties, Microstructure and Processing* 2008;491(1-2):131-6.
- (6) Mughrabi H. Fatigue mechanisms in the ultrahigh cycle regime. 9th International Fatigue Congress Atlanta, USA. May 2006.
- (7) Stanzl-Tschegg S, Mughrabi H, Schuller R. Does Copper Undergo Surface Roughening during Fatigue in the VHC Regime? 16th European Conference of Fracture 2006.
- (8) Kunz L, Lukas P, Svoboda M. Fatigue strength, microstructural stability and strain localization in ultrafine-grained copper. *Materials Science & Engineering A (Structural Materials: Properties, Microstructure and Processing)* 2006 05/25;424(1):97-104.
- (9) Wang QY, Bathias C. Fatigue characterization of a spheroidal graphite cast iron under ultrasonic loading. *J.Mater.Sci.* 2004;39(2):687-689.
- (10) Marines I, Bin X, Bathias C. An understanding of very high cycle fatigue of metals. *Int.J.Fatigue* 2003 22-27 Sept. 2002;25(9):1101-7.
- (11) Bathias C, Drouillac L, Le Francois P. How and why the fatigue S-N curve does not approach a horizontal asymptote. *Int.J.Fatigue* 2001 17-22 Sept. 2000;23:143-51.
- (12) Wang QY, Berard JY, Rathery S, Bathias C. High-cycle fatigue crack initiation and propagation behaviour of high-strength spring steel wires. *Fatigue and Fracture of Engineering Materials and Structures* 1999;22(8):673-677.
- (13) Sohar, C. et al. Gigacycle fatigue behaviour of a high chromium alloyed cold work tool steel. *International Journal of Fatigue* 2007.
- (14) Sakai T, Sato Y, Oguma N. Characteristic S-N properties of high-carbon-chromium-bearing steel under loading in long-life fatigue. *Fatigue and Fracture of Engineering Material and Structures* 2002 08;25(8-9):765-73.

- (15) Mughrabi H. On 'multi-stage' fatigue life diagrams and the relevant life-controlling mechanisms in ultrahigh-cycle fatigue. *Fatigue and Fracture of Engineering Material and Structures* 2002 08;25(8):755-64.
- (16) Billaudeau T, Nadot Y. Support for an environmental effect on fatigue mechanisms in the long life regime. *Int.J.Fatigue* 2004 08;26(8):839-47.
- (17) Paris, P.C. et. al. Fatigue crack growth from small to large cracks in gigacycle fatigue with fish-eye failures. 9th International Fatigue Congress Atlanta, USA, May 2006.
- (18) Murakami Y, Endo M. Effects of defects, inclusions and inhomogeneities on fatigue strength. *Int.J.Fatigue* 1994 04;16(3):163-82.
- (19) Murakami Y, Nagata J. Influence of hydrogen trapped by inclusions on fatigue strength of bearing steel. *Strength, Fracture and Complexity* 2003;1(4):233-4.
- (20) Murakami Y, Nomoto T, Ueda T. Factors influencing the mechanism of superlong fatigue failure in steels. *Fatigue & Fracture of Engineering Materials & Structures* 1999 07;22(7):581-90.
- (21) Murakami Y, Nomoto T, Ueda T, Murakami Y. On the mechanism of fatigue failure in the superlong life regime ( $N > 10^7$  cycles). II. A fractographic investigation. *Fatigue & Fracture of Engineering Materials & Structures* 2000 11;23(11):903-10.
- (22) Murakami Y, Nomoto T, Ueda T, Murakami Y. On the mechanism of fatigue failure in the superlong life regime ( $N > 10^7$  cycles). I. Influence of hydrogen trapped by inclusions. *Fatigue & Fracture of Engineering Materials & Structures* 2000 11;23(11):893-902.
- (23) Murakami Y, Takada M, Toriyama T. Super-long life tension-compression fatigue properties of quenched and tempered 0.46% carbon steel. *Int.J.Fatigue* 1998 10;20(9):661-7.
- (24) Murakami Y, Yokoyama NN, Nagata J. Mechanism of fatigue failure in ultralong life regime. *Fatigue and Fracture of Engineering Material and Structures* 2002 08;25(8):735-46.
- (25) Nagata J, Murakami Y. Factors influencing the formation of ODA in ultralong fatigue regime. *Journal of the Society of Materials Science, Japan* 2003 08;52(8):966-73.
- (26) Murakami Y, Matsunaga H. The effect of hydrogen on fatigue properties of steels used for fuel cell system. *Int.J.Fatigue* 2006 11;28(11):1509-20.
- (27) Murakami Y, Nagata J, Matsunaga H. Factors affecting ultralong fatigue life and design method for components. 9th International Fatigue Congress Atlanta, USA, May 2006.
- (28) Shiozawa K, Morii Y, Nishino S, Lu L. Subsurface crack initiation and propagation mechanism in high-strength steel in a very high cycle fatigue regime. *Int.J.Fatigue* 2006;28(11):1521-1532.

- (29) Shiozawa K, Morii Y, Nishino S. Subsurface crack initiation and propagation mechanism under the super-long fatigue regime for high speed tool steel (JIS SKH51) by fracture surface topographic analysis. *JSME International Journal, Series A: Solid Mechanics and Material Engineering* 2006;49(1):1-10.
- (30) M. Randelius. Influence of microstructure on fatigue and ductility properties of tool steels. Stockholm: Royal Institute of Technology; 2008.
- (31) Paris, P.C. et. al. The relationship of effective stress intensity, elastic modulus and Burgers-vector on fatigue crack growth. *Proceedings of the International Conference on Very High Cycle Fatigue III* Kyoto, Japan. Sep 2004.

# Very high cycle fatigue of engineering materials

---

Many engineering components reach a finite fatigue life well above  $10^9$  load cycles. Some examples of such components are found in airplanes, automobiles or high speed trains. For some materials the fatigue failures have lately been found to occur well after  $10^7$  load cycles, namely in the Very High Cycle Fatigue (VHCF) range. This finding contradicted the established concept of fatigue limit for these materials, which postulates that having sustained  $10^7$  load cycles the material is capable of enduring an infinite number of cycles provided that the service conditions are unchanged.

With the development of modern ultrasonic fatigue testing equipment it became possible to experimentally establish VHCF behaviour of various materials. For most of them the existence of the fatigue limit at  $10^7$  load cycles has been proved wrong and their fatigue strength continues to decrease with increasing number of load cycles. This report describes very long life fatigue properties of most commonly used engineering materials including aluminium, titanium, nickel alloys and various types of steel.